

1 Ozone oxidation of oleic acid surface films decreases aerosol CCN
2 activity

3
4 A. N. Schwier,¹ N. Sareen,¹ T. L. Lathem,² A. Nenes,^{2,3,*} and V. F. McNeill^{1,*}

5
6 ¹Department of Chemical Engineering, Columbia University, New York, New York USA

7
8 ²School of Earth and Atmospheric Sciences, Georgia Institute of Technology, Atlanta, Georgia,
9 USA

10
11 ³School of Chemical and Biomolecular Engineering, Georgia Institute of Technology, Atlanta,
12 Georgia USA

13
14 *to whom correspondence should be addressed.

15 vfm2103@columbia.edu, athanasios.nenes@gatech.edu

16

17

18

19

20

21

22

23

24 ***Abstract***

25 Heterogeneous oxidation of aerosols composed of pure oleic acid ($C_{18}H_{34}O_2$, an unsaturated fatty
26 acid commonly found in continental and marine aerosol) by gas-phase O_3 is known to increase
27 aerosol hygroscopicity and activity as Cloud Condensation Nuclei (CCN). Whether this trend is
28 preserved when the oleic acid is internally mixed with other electrolytes is unknown and
29 addressed in this study. We quantify the CCN activity of sodium salt aerosols (NaCl, Na_2SO_4)
30 internally mixed with sodium oleate (SO) and oleic acid (OA). We find that particles containing
31 roughly one monolayer of SO/OA show similar CCN activity to pure salt particles, whereas a
32 tenfold increase in organic concentration slightly depresses CCN activity. O_3 oxidation of these
33 multicomponent aerosols has little effect on the critical diameter for CCN activation for
34 unacidified particles at all conditions studied, and the activation kinetics of the CCN are similar
35 in each case to those of pure salts. SO-containing particles which are acidified to atmospherically
36 relevant pH before analysis in order to form oleic acid, however, show depressed CCN activity
37 upon oxidation. This effect is more pronounced at higher organic concentrations. The behavior
38 after oxidation is consistent with the disappearance of the organic surface film, supported by
39 Köhler Theory Analysis (KTA). κ -Köhler calculations show a small decrease in hygroscopicity
40 after oxidation. The important implication of this finding is that oxidative aging may not always
41 enhance the hygroscopicity of internally mixed inorganic-organic aerosols.

42

43

44

45

46 **1. Introduction**

47 Surface-active molecules contain both hydrophilic and hydrophobic moieties; therefore, they tend
48 to partition at the gas-liquid interface of aqueous solutions. Given that both water and surface-
49 active organics are ubiquitous in tropospheric aerosols, organic films have long been
50 hypothesized to exist on aerosol surfaces [Ellison et al., 1999; Gill et al., 1983] with potentially
51 important consequences for atmospheric chemistry and climate. Organic films may affect the
52 ability of the aerosol to act as CCN [Andrews and Larson, 1993; Asa-Awuku et al., 2008; Chuang
53 et al., 1997; Ervens et al., 2005; Facchini et al., 1999; Novakov and Penner, 1993; Shulman et
54 al., 1996], ice nuclei [Cziczo et al., 2004; DeMott et al., 2003; Kärcher and Koop, 2005], and alter
55 aerosol optical properties [Bond and Bergstrom, 2006; Dinar et al., 2008; Kanakidou et al., 2005;
56 Malm and Kreidenweis, 1997; Mircea et al., 2005]. These films may act as a barrier to mass
57 transport across the gas-liquid interface, with implications for aerosol heterogeneous
58 chemistry [Folkers et al., 2003; McNeill et al., 2006; Thornton and Abbatt, 2005] and the rate of
59 water uptake [Asa-Awuku et al., 2009; Cruz and Pandis, 2000; Demou et al., 2003; Garland et
60 al., 2005; Gill et al., 1983; Hemming and Seinfeld, 2001; Nenes et al., 2002; Rubel and Gentry,
61 1984; Rudich et al., 2000; Saxena and Hildemann, 1997]. Surface-active organics can impact
62 CCN activity by lowering aerosol surface tension, thus affecting the Kelvin term of the Köhler
63 equation [Shulman et al., 1996], but they can also affect the Raoult term by altering n_s , the
64 number of moles of solute, especially when surface-bulk partitioning of solute is taken into
65 account [Kokkola et al., 2006; Sorjamaa et al., 2004; Sorjamaa and Laaksonen, 2006].

66

67 Oleic acid ($C_{18}H_{34}O_2$), a surface-active monounsaturated long-chain fatty acid, has been detected
68 in urban, rural and marine aerosols [Cheng and Li, 2005; Graham et al., 2003; Kawamura et al.,

69 2003; Limbeck and Puxbaum, 1999; Robinson et al., 2006; Schauer et al., 1996, 2002; Simoneit
70 et al., 2004; Stephanou and Stratigakis, 1993; Yue and Fraser, 2004]. It is the most common
71 fatty acid found in plant membranes, is prevalent in many cooking oils, and it is used as a marker
72 for meat cooking aerosols[Rogge et al., 1991].Ozonolysis of oleic acid yields nonanal, nonanoic
73 acid, 9-oxononanoic acid, and azelaic acid under humid conditions, and high molecular weight
74 products under dry conditions[Hearn et al., 2005; Hearn and Smith, 2004; Katrib et al., 2005a;
75 McNeill et al., 2007; Rudich et al., 2007; Smith et al., 2002; Thornberry and Abbatt, 2004; Vesna
76 et al., 2008, 2009; Zahardis et al., 2005, 2006a; Zahardis and Petrucci, 2007].Under
77 atmospherically-relevant conditions, nonanal primarily partitions to the gas phase, while the
78 other products remain in the condensed phase. Due to the importance of oleic acid as a
79 tracer species[Rogge et al., 1991] and its relatively well-understood O₃ oxidation mechanism,
80 many studies of the kinetics of oleic acid oxidation have been performed on systems of varying
81 morphology, including pure oleic acid particles[Broekhuizen et al., 2004b; Hearn et al., 2005;
82 Hearn and Smith, 2004; Hung et al., 2005; Katrib et al., 2005a; Lee and Chan, 2007; Morris et
83 al., 2002; Pfrang et al., 2010; Reynolds et al., 2006; Sage et al., 2009; Smith et al., 2002; Vesna
84 et al., 2008; Zahardis et al., 2005, 2006a, 2006b; Ziemann, 2005], mixed organic particles[Hearn
85 and Smith, 2005; Hung and Ariya, 2007; Nash et al., 2005], films on polystyrene beads[Katrib et
86 al., 2004, 2005b], films on aqueous sea salt aerosol[King et al., 2004], films in coated wall flow
87 tube studies[de Gouw and Lovejoy, 1998; Knopf et al., 2005; Moise and Rudich, 2000, 2002;
88 Thornberry and Abbatt, 2004], and films on crystal surfaces[Asad et al., 2004].

89

90 Pure organic aerosols are generally less hygroscopic and CCN active than deliquescent inorganic
91 particles (such as NaCl or (NH₄)₂SO₄)[Petters and Kreidenweis, 2007]. Oxidation of organic

92 aerosol material can increase the number of polar, hydrophilic functional groups present in the
93 condensed phase, potentially leading to increased hygroscopicity and CCN activity. Oleic acid
94 particles have been used extensively as a model system to study the effect of oxidation on the
95 CCN activity of organic particles. *Kumar et al.*[2003] created pure oleic acid particles through
96 homogenous nucleation and observed no activation for particle sizes up to 140 nm and $\leq 0.6\%$
97 supersaturation (SS). *Abbatt et al.*[2005] studied the CCN activity of ammonium sulfate aerosols
98 coated with oleic acid and found that particles with thin (~ 2.5 -5 nm) coatings of oleic acid were
99 not CCN active, but that CCN activity increased when the organic mole fraction increased. This
100 somewhat counterintuitive result was attributed to the fact that the particle diameter increased
101 with increasing organic mass fraction, reducing the magnitude of the Kelvin effect. *Broekhuizen*
102 *et al.*[2004a] found that oxidation products of oleic acid (nonanoic acid and azelaic acid) were
103 highly CCN active. In a separate study, they found that CCN activity was enhanced after
104 oxidation for both pure oleic acid particles and particles formed by atomizing a solution of oleic
105 acid in methanol [*Broekhuizen et al.*, 2004b]. The enhancement in CCN activity occurred at very
106 high ozone exposures (~ 0.4 atms) for pure oleic acid particles, and at atmospherically relevant
107 exposures ($< 1 \times 10^{-4}$ atms) for the oleic acid/methanol particles. *Shilling et al.*[2007] determined
108 that 200 nm mobility diameter oleic acid particles, generated through either homogenous
109 nucleation or atomization, became CCN active at $0.66(\pm 0.06)\%$ supersaturation after exposure to
110 greater than 0.01 atms O_3 .

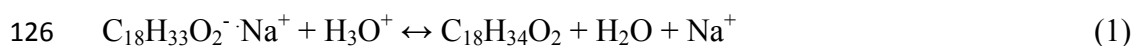
111

112 Despite its atmospheric relevance, the response of mixed inorganic/oleic acid particles to
113 oxidation has not been considered in published CCN activity studies. This is an important
114 omission, because the acid almost always coexists in the atmosphere with inorganic salts. Little

115 is known about the interactions of oleic acid and its oxidation products with water in a high ionic
116 strength environment. These issues are addressed in this study. An aerosol flow tube reactor
117 coupled with a continuous flow cloud condensation nucleus counter is used to examine the effect
118 of ozone oxidation on the CCN activity of aerosol particles containing mixtures of sodium oleate
119 (SO)/oleic acid (OA) with inorganic salts (NaCl or Na₂SO₄).

120 **2. Methods**

121 **2.1. Experimental.** Sodium oleate (C₁₈H₃₃O₂⁻ Na⁺), the sodium salt of oleic acid (C₁₈H₃₄O₂), has
122 much higher solubility in water than oleic acid. It was used in these experiments to simplify the
123 preparation of aerosols containing a small, controlled amount of organic material. When the pH
124 of aerosols containing SO is lowered to atmospherically relevant values via acidification (see
125 details below), the oleate ion converts to oleic acid according to:



127

128 For the experiments performed, the setup is shown in Figure 1. Polydisperse submicron aerosols
129 were generated using a constant output atomizer (TSI 3076). Atomizer solutions were prepared
130 using Millipore water with 0.001 M or 0.01 M SO (Sigma Aldrich) and 0.05 M NaCl. This
131 technique, using 0.001 M SO, was used by *McNeill et al.*[2007] to generate aerosols with an
132 inferred population-averaged oleate surface coverage of ~92%. The atomizer output was
133 combined with a humidified N₂ dilution stream. This combined stream was sent through an
134 aerosol flow tube reactor (7.5 cm ID, 55 cm length). Relative humidity was measured at the
135 outlet of the flow tube reactor using a commercial hygrometer (Vaisala) and was maintained
136 between 62-67%. Ozone was generated by flowing O₂ in an N₂ carrier stream through a

137 photoreactor containing a Hg lamp (Jelight, Inc.). This stream entered the flow tube reactor
138 through a moveable stainless steel injector tube. Ozone concentrations of 0.2 and 1 ppm were
139 used. Total flow through the reactor was 0.8 LPM, with a reaction time of 3 minutes. Processed
140 aerosols in the reactor effluent flowed through a diffusion drier before being characterized by a
141 Differential Mobility Analyzer (DMA, TSI 3080), a Condensation Particle Counter (CPC, TSI
142 3775) and a Continuous Flow Streamwise Thermal Gradient CCN Chamber (CFSTGC, Droplet
143 Measurement Technologies) [Lance *et al.*, 2006; Roberts and Nenes, 2005]. Aerosols were size-
144 selected using the DMA, and the DMA output flow was split between the CPC and the CFSTGC.
145 0.8 LPM entered the DMA and split 0.5 LPM to the CFSTGC, 0.3 LPM to the CPC. Scanning
146 Mobility CCN Analysis [Moore *et al.*, 2010] was used to determine the size-resolved CCN
147 activity of the aerosol, where the voltage applied to the DMA is scanned so that a complete
148 activation curve (fraction of classified particles acting as CCN) is obtained every 2 minutes. The
149 average total aerosol number concentration in the reactor output was $9.6 \pm 2.0 \times 10^4 \text{ cm}^{-3}$. The size
150 distribution of NaCl particles had a geometric surface area-weighted mean particle diameter of
151 $202 \pm 7 \text{ nm}$ with a geometric standard deviation of 1.59. Na_2SO_4 particles had a particle diameter
152 of $194 \pm 5 \text{ nm}$ with a geometric standard deviation of 1.63.

153

154 A second series of experiments was performed in order to test the sensitivity of CCN activity in
155 the mixed inorganic-SO aerosols to particle pH because atmospheric aerosols are typically
156 acidic [Keene *et al.*, 2004; Zhang *et al.*, 2007]. Under acidic conditions oleate exists in its un-
157 ionized, lower-solubility form, oleic acid, according to Reaction 1. The atomizer output was
158 passed over an H_2SO_4 reservoir before combining with humidified N_2 and entering the flow tube
159 reactor. Assuming an uptake coefficient $\gamma = 0.5$ [ten Brink, 1998], an aerosol surface area of $S_a = 6.2$

160 $\pm 1.4 \times 10^{-5} \text{ cm}^2 \text{ cm}^{-3}$, geometric volume-weighted mean diameter $D_p = 232 \text{ nm}$, and a residence time
161 of $\sim 0.8 \text{ s}$ in the H_2SO_4 reservoir, we estimate that the particles are acidified from an initial $\text{pH} = 8$
162 to $\text{pH} \sim 0.4$. The calculation methodology is shown in the supplementary material. Given that
163 the pK_a of oleic acid = 5.02 [Riddick *et al.*, 1986] and $\text{pH} = 0.4$, the ratio of oleate to non-
164 dissociated oleic acid in the particles ($[\text{C}_{18}\text{H}_{33}\text{O}_2^-]/[\text{C}_{18}\text{H}_{34}\text{O}_2]$) = 2.3988×10^{-5} , that is, nearly all
165 of the organic will be present as oleic acid under these conditions. For the acidification
166 experiments the total aerosol number concentration was $9.9 \pm 1.4 \times 10^4 \text{ cm}^{-3}$.

167
168 The following control experiments were also performed: “pure” sodium oleate particles were
169 generated by atomizing an aqueous solution of 0.001 M SO. In order to investigate possible
170 variations in pH buffering by different counterions, experiments were also performed using
171 aerosols atomized from solutions containing 0.001 M or 0.01 M SO and 0.06 M Na_2SO_4 . Finally,
172 pure inorganic aerosols prepared from solutions containing 0.05 M NaCl or 0.06 M Na_2SO_4 were
173 oxidized with 1 ppm O_3 in the flow tube reactor, showing no significant deviation in CCN
174 activity from the pure salt calibrations without oxidation.

175
176 **2.2 Data Analysis.** Köhler Theory provides the framework used to describe cloud droplet
177 formation from activation of soluble particles [Cruz and Pandis, 1997; Gerber *et al.*, 1977; Katz
178 and Kocmond, 1973]. A single-parameter expression of Köhler theory, referred to as κ -Köhler
179 theory, was introduced by Petters and Kreidenweis [2007] to account for the effect of variations in
180 solute hygroscopicity on CCN activity. Values of the hygroscopicity factor, κ , of $0.5 < \kappa < 1.4$ are
181 typical for inorganic particles in the atmosphere. For hygroscopic organic particles, $0.01 < \kappa < 0.5$,

182 whereas for non-hygroscopic materials (including highly hydrophobic organics) approaches
 183 zero. κ is derived from the CCN activity data as follows [Petters and Kreidenweis, 2007],

$$184 \quad \kappa = \frac{4A^3}{27d_d^3 \ln^2 S} \quad (2)$$

$$185 \quad \text{where } A = \frac{4\sigma_{s/a} M_w}{RT\rho_w} \quad (3)$$

186
 187 Here, d_d is the critical dry activation diameter of the particle [m] (determined from CCN
 188 activation experiments), S is the water saturation ratio ($S = 1 + 0.01S_c$, where S_c is critical
 189 supersaturation [%]), $\sigma_{s/a}$ is the surface tension of water at the surface/air interface at the median
 190 temperature of the CFSTGC column, M_w is the molecular weight of water, R is the universal gas
 191 constant, T is the median temperature of the CFSTGC column [K], and ρ_w is the density of water.

192
 193 Köhler Theory Analysis (KTA) was also used to infer the surface tension of the mixed aerosol
 194 before and after oxidation [Padro et al., 2007]. The following equations were used [Padro et al.,
 195 2007]:

$$196 \quad \frac{M_o}{\rho_o} = \frac{\varepsilon_o \nu_o}{\frac{256}{27} \left(\frac{M_w}{\rho_w}\right)^2 \left(\frac{1}{RT}\right)^3 \sigma_{s/a}^3 \omega^{-2} - \frac{\rho_i}{M_i} \varepsilon_i \nu_i} \quad (4)$$

$$197 \quad \text{where } \varepsilon_i = \frac{\frac{m_i}{\rho_i}}{\frac{m_i}{\rho_i} + \frac{m_o}{\rho_o}} \quad (5)$$

198 Here, M_o , M_i , ρ_o and ρ_i refer to the average molecular weight and density of the organic and
 199 inorganic components of the aerosol, while ν_o and ν_i are effective van't Hoff factors, ε_o and ε_i are
 200 volume fractions, and m_o , m_i are the mass fractions of the organic and inorganic components,

201 respectively. The fitted CCN activity factor, ω , is determined from the log-log plots of
202 S_c versus d_d , fit to the equation [Asa-Awuku *et al.*, 2010],

$$203 \quad S_c = \omega d_d^{-3/2} \quad (6)$$

204 κ and ω are related by $\omega = (4A^3 / 27\kappa)^{1/2}$.

205 **3. Results**

206 The results of our CFSTGC measurements for the SO/OA/NaCl and SO/OA/Na₂SO₄ systems are
207 shown in Figures 2-5. A complete list of calculated κ values (derived from eqs. (2) and (3)) and
208 power law exponents for the CCN activity data is available in the supplementary material.

209

210 **3.1 SO/NaCl.** As expected, pure SO/H₂O aerosols are much less CCN active than NaCl aerosols
211 (Figure S1), with $\kappa = 0.12 \pm 0.004$. As shown in Figures 2a and S1, the CCN activity of mixed
212 SO/NaCl particles generated from 0.001 M SO/0.05 M NaCl solutions ($\kappa = 1.19 \pm 0.03$) is similar
213 to that of pure NaCl particles. The mixed particles with higher SO content show intermediate
214 CCN activity ($\kappa = 0.87 \pm 0.06$) compared to particles with lower SO content and pure SO/H₂O
215 particles. The mixed SO/NaCl aerosols exhibit similar wet activated diameter profiles to NaCl
216 particles (Figure 2b), indicating that the presence of oleate does not retard the activation kinetics
217 of the aerosol on the timescale of the CCN measurements [Engelhart *et al.*, 2008; Moore *et al.*,
218 2008]. Furthermore, for all these systems the critical supersaturation shows a power law
219 dependence of $S_c \sim d_d^{-1.42 \pm 0.04}$, suggesting that the CCN activity of these particles is described
220 fairly well by Köhler theory, with no significant solubility limitations or size-dependent surface-
221 bulk partitioning effects. For a system that is perfectly described by Köhler Theory, we expect
222 the relationship to follow $S_c \sim d_d^{-1.5}$, as shown in eq. (6) [Padro *et al.*, 2007].

223

224 CCN activity did not significantly change upon exposure to O₃ for the unacidified mixed SO/NaCl
225 aerosols studied. Critical dry diameters changed by ~0.5% for the particles generated from 0.001
226 M SO/0.05 M NaCl solutions and ~1.6% for the particles generated from 0.01 M SO/0.05 M
227 NaCl solutions (Figure 2a); this leads to a change of particle critical supersaturation by ~1% for
228 the former and ~3% for the latter. The change in CCN activity due to oxidation effectively falls
229 within the standard deviation of the non-oxidized data, showing relatively little effect of
230 oxidation to unacidified mixed SO/NaCl particles. Calculated κ values after oxidation for all
231 SO/NaCl aerosols were similar to the κ values prior to oxidation; $\kappa = 1.14 \pm 0.02$ for 0.001 M
232 SO/0.05 M NaCl and $\kappa = 0.83 \pm 0.04$ for 0.01 M SO/0.05 M NaCl. The change in CCN activity
233 was not dependent on the concentration of ozone used within the range studied here (0.2 – 1
234 ppm). The wet diameter profiles after oxidation are nearly identical to the non-oxidized SO/NaCl
235 particle wet diameters. This suggests that surface films, if present, do not retard CCN activation
236 kinetics and growth.

237

238 **3.2 SO/Na₂SO₄.** Because oleate oxidation generates organic acid products, it is possible that the
239 particle pH changes during oxidation, with implications for fatty acid solubility [Cistola *et al.*,
240 1988]. In the unacidified SO/NaCl system, the formation of organic acid oxidation products may
241 result in the formation, and possible subsequent volatilization, of HCl, due to its high vapor
242 pressure. The net pH change is expected to differ in the SO/Na₂SO₄ system. The CCN activity
243 data for the SO/Na₂SO₄ experiments are shown in Figure 3.

244

245 The CCN activity of the SO/Na₂SO₄ particles follows trends similar to what we observed for the
246 SO/NaCl particles. The CCN activity of the particles generated from 0.001 M SO/0.06 M
247 Na₂SO₄ solutions ($\kappa = 0.71 \pm 0.04$) and 0.01 M SO/0.06 M Na₂SO₄ solutions ($\kappa = 0.68 \pm 0.03$) is
248 roughly similar to that of pure Na₂SO₄ particles. The CCN activity changes little upon oxidation,
249 and the resulting hygroscopic parameters ($\kappa = 0.71 \pm 0.02$ and $\kappa = 0.67 \pm 0.03$, respectively) are
250 similar to the non-oxidized SO/Na₂SO₄ particles, analogous to our observations for the
251 SO/NaCl system. The wet diameter profiles are again very similar both before and after
252 oxidation, suggesting that there is no kinetic limitation to water uptake.

253

254 **3.3 Acidified experiments: OA/NaCl and Na₂SO₄.** As an additional test of the effect of pH on
255 our observations of CCN activity for the SO/NaCl and SO/Na₂SO₄ systems, we performed a set
256 of experiments in which the atomized mixed particles were exposed to gas-phase H₂SO₄ before
257 oxidation. The goal of these experiments was to create a particle with a low pH typical of that of
258 atmospheric aerosols, conditions under which sodium oleate and the organic acid oxidation
259 products are in their un-ionized, lower-solubility forms (cf. Reaction (1)). As demonstrated in
260 Section 2, nearly all of the SO will be present as oleic acid under these conditions. The results of
261 these experiments are shown in Figure 4 and 5.

262

263 The CCN activity of acidified 0.001 M SO/0.05 M NaCl ($\kappa = 1.14 \pm 0.05$) and 0.01 M SO/0.05 M
264 NaCl ($\kappa = 0.97 \pm 0.08$) decreased after oxidation ($\kappa = 1.07 \pm 0.05$ and 0.79 ± 0.02 , respectively),
265 more noticeably at higher instrument supersaturations and SO concentrations (Figure 4 and
266 inset). The wet activated diameters do not show any kinetic limitations to water uptake.

267 Similarly, the acidified SO/Na₂SO₄ data shows similar CCN activity behavior to the acidified
268 SO/NaCl particles (Figure 5). The hygroscopicity values for both 0.001 M and 0.01 M SO/0.06
269 M Na₂SO₄ decrease after oxidation, and both follow the power law dependence expected from
270 Köhler theory (where $S_c \sim d_d^{-1.46 \pm 0.005}$ and $S_c \sim d_d^{-1.37 \pm 0.002}$, respectively).

271

272 **3.4 Köhler Theory Analysis.** The parameters and results of the KTA calculations can be seen in
273 Tables 1-3. The initial in-particle concentrations of oleate and the inorganic salt were calculated
274 following *McNeill et al.*[2007]. After oxidation, we assume the oleate is completely oxidized to
275 form nonanal and azelaic, nonanoic, and 9-oxononanoic acids. The product yields reported
276 by *Vesna et al.*[2009] were used. The density of 9-oxononanoic acid is unknown and was
277 assumed to be 1 g cm⁻³. The inorganic effective van't Hoff parameter (ν_i), T , the fitted CCN
278 activity factor (ω), and ρ_w all varied with varying S_c and d_d . To account for dissociation of the
279 organics, $\nu_o = 1$ and 2 were tested, but the results for both salts at varying ozone concentrations,
280 regardless of the ν_o used, were the same to within 3%; the data for $\nu_o = 2$ is shown.

281

282 The results suggest that the surface tension of the aerosols increases slightly after oxidation,
283 which is consistent with the breakup of the oleate monolayer (we have measured the surface
284 tension of bulk solutions saturated in NaCl and SO using pendant drop tensiometry to be $44.4 \pm$
285 0.8 dyn cm⁻¹). The calculated surface tension values after oxidation fall between 64-75 dyn cm⁻¹,
286 slightly less than the surface tension of saturated NaCl and Na₂SO₄ solutions [*Washburn,*
287 *2003*]. *Vesna et al.*[2009] found that a large portion of the aerosol organic mass after oleic acid
288 oxidation consisted of unidentified products (UP). Including these products in our KTA

289 calculations (assuming an average molar mass of 500 g mol⁻¹ and density of 1.4 g cm⁻³, [Turpin
290 and Lim, 2001]), gave very similar surface tension results compared to when only the 4 main
291 oxidation species are considered. Therefore, the single-phase approximation represents our
292 system well.

293

294 **4. Discussion**

295 The particles generated using 0.001 M SO atomizer solutions were designed such that the
296 particles with the surface-area weighted average diameter would be covered with approximately
297 1 monolayer of oleate/OA at 65% RH. Following McNeill *et al.* [2006], we estimated the
298 organic fractional coverage of the total available surface area of our aerosol population by,

$$299 \quad \Theta = \frac{\sum_i \theta_i N_i}{\sum_i N_i} \quad (7)$$

300 where θ_i and N_i are the fractional surface coverage of the aerosol and the number density in the
301 DMA size bin i , and Θ is the overall fractional surface coverage. Assuming three things: that all
302 the organic partitions to the surface until saturated coverage is reached, that it is equally
303 distributed across the aerosol population in constant proportion to either NaCl or Na₂SO₄, and an
304 oleate footprint of 48 Å² [Langmuir, 1917], we find that for the particles generated using 0.001 M
305 SO/0.05 M NaCl or 0.001 M SO/0.06 M Na₂SO₄ atomizer solutions, $\Theta \approx 0.83$ (83% overall
306 surface coverage) and $\Theta \approx 1.01$ (100%), respectively. This calculation also implies that smaller
307 particles with larger surface area-to-volume ratios will not contain enough oleate for full
308 monolayer coverage, while the larger particles will have complete monolayer coverage. There is
309 indirect evidence of monolayer formation at similar conditions from N₂O₅ uptake experiments by

310 *McNeill et al.*[2007]. In addition, *McNeill et al.*[2007] analyzed SO/NaCl particles formed using
311 this technique by SEM-EDAX, which showed the existence of uniform coatings of SO on the
312 particles. Using kinetic data from *McNeill et al.*[2007], we calculate the extent of oxidation in
313 particles with lower SO content to be 76-100%, varying with O₃ concentration. The reacto-
314 diffusive length in the OA-O₃ system is ~20 nm, so for particles with higher SO content, the
315 kinetic model of *Smith et al.* [2002], for reactions occurring in a near-surface layer of a pure
316 oleic acid particle, can be applied. Using their kinetic model and parameters, we calculate ~100%
317 oxidation.

318 Several studies on bulk systems have shown that when an oleic acid monolayer at the air-
319 aqueous interface is exposed to ozone, the organic film breaks down, as evidenced by a decrease
320 in surface pressure [*González-Labrada et al.*, 2006, 2007], disappearance of the vibrational sum
321 frequency generation signal [*Voss et al.*, 2006, 2007], or neutron reflection [*King et al.*, 2009].
322 From these studies, it appears that the oxidation products leave the gas-particle interface soon
323 after oxidation. Nonanoic acid, 9-oxononanoic acid, and azelaic acid are more soluble in water
324 than oleic acid, and they may partition into the aqueous solution after they are formed. However,
325 there is evidence that azelaic acid [*Tuckermann*, 2007; *Tuckermann and Cammenga*, 2004] and
326 nonanoic acid [*Caetano et al.*, 2007; *Gilman et al.*, 2004; *King et al.*, 2009] are surface-active and
327 CCN active [*Broekhuizen et al.*, 2004a]. *McNeill et al.*[2007] observed that nonanoic acid in wet
328 NaCl aerosols, in the absence of other oleic acid oxidation products, was volatile at room
329 temperature. Nonanal has been reported to enter the gas phase after it is formed [*Katrib et al.*,
330 2004; *Moise and Rudich*, 2002; *Thornberry and Abbatt*, 2004; *Voss et al.*, 2006; *Wadia et al.*,
331 2000]. *Hung and Ariya*[2007] analyzed the oxidation of mixed OA/NaCl particles using ATR-
332 FTIR, and showed that before oxidation, while increasing RH, there was no increase in the water

333 content of the particles, but after oxidation, there was an initial increase, then decrease in the
334 liquid water content. They determined that the hygroscopicity of OA/NaCl particles changed
335 after oxidation, but could vary and was affected by relative humidity levels. *King et al.*[2009]
336 used neutron scattering and surface pressure measurements to study the disappearance of an oleic
337 acid surface film on an aqueous subphase upon exposure to O₃. They observed that roughly half
338 of the oxidation products remained at the surface, while the remainder were either released into
339 the gas phase or incorporated into the bulk. Consistent with our observations that CCN activity
340 was not enhanced compared to the pure salt for the particles generated using 0.001 M SO/0.05 M
341 NaCl or 0.001 M SO/0.06 M Na₂SO₄ atomizer solutions, they calculated, using Köhler theory,
342 that one monolayer of oleic acid on a 100 nm radius particle would not depress surface tension
343 during cloud droplet formation enough to affect the critical supersaturation point of the droplet.
344 Based on the assumption that the oleic acid oxidation would be complete and would lead to a
345 surface film of nonanoic acid, with azelaic acid dissolving into the bulk phase, they predicted
346 that the oxidation of an oleic acid surface film on an aerosol particle would decrease the critical
347 supersaturation required for droplet formation, increasing CCN activity. Surface-bulk
348 partitioning was not taken into account in that calculation[*Kokkola et al.*, 2006; *Sorjamaa et al.*,
349 2004; *Sorjamaa and Laaksonen*, 2006].

350

351 Our KTA calculations show support for a small increase in particle surface tension upon
352 oxidation. Such an increase in surface tension could occur with the disappearance of a surfactant
353 film at the interface. However, our observation that the mixed inorganic/organic particles become
354 more organic-like in their CCN activity after oxidation is not inconsistent with the oxidation
355 products remaining at the interface. The high salt content of the particles prior to activation and

356 the acidic conditions would decrease the solubility of the oxidation products in these aerosols as
357 compared to the bulk films studied by other groups, possibly leading to phase separation. If
358 oxidation of an oleate surface layer is complete, it would result in the doubling of the number of
359 organic molecules present at the interface. In the absence of external pressure, oleate forms
360 expanded-state monolayers on aqueous surfaces, that is, the surface layer formed by the
361 hydrophobic tail groups is not well-ordered[Rideal, 1925; Schofield and Rideal, 1926].
362 Immediately after forming, the oxidation products exist in a disordered double layer until they
363 dissolve into the bulk or are released into the gas phase, or sufficient water is taken up by the
364 particle to dissolve them. Transport to and self-assembly of surfactant products at the interface
365 may be slow after oxidation, occurring on timescales much longer than the residence time in our
366 experimental system[Lass *et al.*, 2010; McIntire *et al.*, 2010]. The work of McIntire *et*
367 *al.*[2010]on the ozonolysis of alkene self-assembled monolayers (SAMs) with internal double
368 bonds provides support for the formation of a complex, low-hygroscopicity organic surface layer
369 upon ozonolysis. They reported that ozonolysis did not increase the hygroscopicity of surface-
370 bound alkenes, and it was hypothesized that the polar head groups of the oxidation products were
371 buried in a mixed organic layer after oxidation rather than at the air-organic interface. They
372 concluded that the three-dimensional structure of particles was critical for predicting aerosol
373 hygroscopicity and CCN activity.

374

375 For internal mixtures, κ can be described by a weighted linear sum of the components in the
376 system [Petters and Kreidenweis, 2007]. κ of azelaic acid was found to be ~ 0.1 , while κ of the
377 other oxidation products is unknown. If we assume that κ for all oxidation products is 0.1 and
378 use the weighted sum approach, we find that the theoretical κ values after oxidation from 0.001

379 M SO/0.05 M NaCl and 0.001 M SO/0.06 M Na₂SO₄ are 1.23 and 0.83, respectively. Possible
380 sources of error include the assumption of one κ value for the four main oxidation products. The
381 small difference between these theoretical κ values and our observations ($\kappa = 1.19$ and 0.71 ,
382 respectively) suggests that these particles can be accurately described as internally well-mixed.

383

384 Since most of the expected oleate ozonolysis products are organic acids, a change in aerosol pH is
385 possible upon oxidation in the unacidified particles. Due to the possible formation of sodium
386 salts as well as organic acids, this maximum pH change assumes that only the three soluble
387 organic acid oleate oxidation products are formed and dissolve in the aqueous phase. Using the
388 pK_a of each acid (azelaic acid (pK_a=4.55), nonanoic acid (4.95), 9-oxononanoic acid (assumed
389 to be 4.95)), we can estimate the concentration of [H⁺] in our system after oxidation. The
390 calculation methodology is shown in the supplementary material. Assuming pH = 8 initially and
391 using product yields from *Vesna et al.* [2009], after complete oxidation of an aerosol with in-
392 particle oleate concentration of 0.176 M [McNeill et al., 2007], the particles would have [H⁺] =
393 1.38 mM, resulting in a final pH of ~3. This pH change is expected to be less in the SO/Na₂SO₄
394 system due to buffering by SO₄²⁻, and negligible in the acidified particles. Fatty acid solubility
395 increases with increasing pH (basic conditions), complementing our observation that CCN
396 activity decreases upon oxidation for acidified particles but shows little change for unacidified
397 particles. This highlights the importance of using atmospherically relevant pH in laboratory
398 studies involving fatty acid surface-bulk partitioning in aerosols. The activated droplet diameters
399 of the studied systems did not change after oxidation; this suggests that if there are any kinetic
400 barriers to hygroscopic growth in these systems, they may be due to the finite dissolution
401 timescale and not a water uptake barrier from the action of the organic surface layer.

402 **5. Conclusions**

403 We examined the effect of ozone oxidation on the CCN activity of aerosol particles containing
404 mixtures of sodium oleate (SO)/oleic acid (OA) with inorganic salts (NaCl or Na₂SO₄). Exposure
405 to O₃ led to decreased CCN activity for particles at atmospherically relevant pH. Wet (activation)
406 diameters of these particles were not significantly different from inorganic calibration standards,
407 suggesting that the activation kinetics are not affected by organic surface films. KTA indicates a
408 slight increase in particle surface tension upon oxidation, consistent with breakup of the organic
409 film after oxidation. The κ values were calculated here for a reaction timescale of up to 3 minutes,
410 and might not accurately represent the real water uptake properties of an aged atmospheric
411 particle. We find that oxidative aging of mixed inorganic-organic aerosols may negatively affect
412 their hygroscopicity and CCN ability.

413 **Acknowledgements**

414 This work was funded by the NASA Tropospheric Chemistry program (grant NNX09AF26G)
415 and the ACS Petroleum Research Fund (grant 48788-DN14). AN acknowledges support from a
416 NSF CAREER grant, and TLL acknowledges support from a NSF Graduate Student Fellowship
417 and a GT Institutional Fellowship.

418

419

420

- 421
422 Reference List
423
- 424 Abbatt, J. P. D., K. Broekhuizen, and P. P. Kumar (2005), Cloud condensation nucleus activity
425 of internally mixed ammonium sulfate/organic acid aerosol particles, *Atmospheric*
426 *Environment*, 39, 4767-4778, doi:10.1016/j.atmosenv.2005.04.029.
- 427 Andrews, E. and S. M. Larson (1993), Effect of Surfactant Layers on the Size Changes of
428 Aerosol-Particles As A Function of Relative-Humidity, *Environmental Science &*
429 *Technology*, 27, 857-865, doi:10.1021/es00042a007.
- 430 Asa-Awuku, A., G. J. Engelhart, B. H. Lee, S. N. Pandis, and A. Nenes (2009), Relating CCN
431 activity, volatility, and droplet growth kinetics of beta-caryophyllene secondary organic
432 aerosol, *Atmospheric Chemistry and Physics*, 9, 795-812, doi:10.5194/acp-9-795-2009.
- 433 Asa-Awuku, A., A. Nenes, S. Gao, R. C. Flagan, and J. H. Seinfeld (2010), Water-soluble SOA
434 from Alkene ozonolysis: composition and droplet activation kinetics inferences from
435 analysis of CCN activity, *Atmospheric Chemistry and Physics*, 10, 1585-1597,
436 doi:10.5194/acp-10-1585-2010.
- 437 Asa-Awuku, A., A. P. Sullivan, C. J. Hennigan, R. J. Weber, and A. Nenes (2008), Investigation
438 of molar volume and surfactant characteristics of water-soluble organic compounds in
439 biomass burning aerosol, *Atmospheric Chemistry and Physics*, 8, 799-812,
440 doi:10.5194/acp-8-799-2008.
- 441 Asad, A., B. T. Mmereki, and D. J. Donaldson (2004), Enhanced uptake of water by oxidatively
442 processed oleic acid, *Atmospheric Chemistry and Physics*, 4, 2083-2089,
443 doi:10.5194/acp-4-2083-2004.
- 444 Bond, T. C. and R. W. Bergstrom (2006), Light Absorption by Carbonaceous Particles: An
445 Investigative Review, *Aerosol Science and Technology*, 40, 27-67,
446 doi:10.1080/02786820500421521.
- 447 Broekhuizen, K., P. P. Kumar, and J. P. D. Abbatt (2004a), Partially soluble organics as cloud
448 condensation nuclei: Role of trace soluble and surface active species, *Geophysical*
449 *Research Letters*, 31, L01107, doi:10.1029/2003GL018203.
- 450 Broekhuizen, K. E., T. Thornberry, P. P. Kumar, and J. P. D. Abbatt (2004b), Formation of cloud
451 condensation nuclei by oxidative processing: Unsaturated fatty acids, *Journal of*
452 *Geophysical Research-Atmospheres*, 109, doi:10.1029/2004JD005298.
- 453 Caetano, W., P. S. Haddad, R. Itri, D. Severino, V. C. Vieira, M. S. Baptista, A. P. Schröder, and
454 C. M. Marques (2007), Photo-Induced Destruction of Giant Vesicles in Methylene Blue
455 Solutions, *Langmuir*, 23, 1307-1314, doi:10.1021/la061510v.

- 456 Cheng, Y. and S. M. Li (2005), Nonderivatization analytical method of fatty acids and cis-
457 pinonic acid and its application in ambient PM_{2.5} aerosols in the greater Vancouver area
458 in Canada, *Environmental Science & Technology*, 39, 2239-2246,
459 doi:10.1021/es030634g.
- 460 Chuang, P. Y., R. J. Charlson, and J. H. Seinfeld (1997), Kinetic limitations on droplet formation
461 in clouds, *Nature*, 390, 594-596, doi:10.1038/37576.
- 462 Cistola, D. P., J. A. Hamilton, D. Jackson, and D. M. Small (1988), Ionization and Phase-
463 Behavior of Fatty-Acids in Water - Application of the Gibbs Phase Rule, *Biochemistry*,
464 27, 1881-1888, doi:10.1021/bi00406a013.
- 465 Cruz, C. N. and S. N. Pandis (1997), A study of the ability of pure secondary organic aerosol to
466 act as cloud condensation nuclei, *Atmospheric Environment*, 31, 2205-2214,
467 doi:10.1016/S1352-2310(97)00054-X.
- 468 Cruz, C. N. and S. N. Pandis (2000), Deliquescence and hygroscopic growth of mixed inorganic-
469 organic atmospheric aerosol, *Environmental Science & Technology*, 34, 4313-4319,
470 doi:10.1021/es9907109.
- 471 Cziczo, D. J., P. J. DeMott, S. D. Brooks, A. J. Prenni, D. S. Thomson, D. Baumgardner, J. C.
472 Wilson, S. M. Kreidenweis, and D. M. Murphy (2004), Observations of organic species
473 and atmospheric ice formation, *Geophysical Research Letters*, 31,
474 doi:10.1029/2004GL019822.
- 475 de Gouw, J. A. and E. R. Lovejoy (1998), Reactive uptake of ozone by liquid organic
476 compounds, *Geophysical Research Letters*, 25, 931-934, doi:10.1029/98GL00515.
- 477 DeMott, P. J., D. J. Cziczo, A. J. Prenni, D. M. Murphy, S. M. Kreidenweis, D. S. Thomson, R.
478 Borys, and D. C. Rogers (2003), Measurements of the concentration and composition of
479 nuclei for cirrus formation, *Proceedings of the National Academy of Sciences of the*
480 *United States of America*, 100, 14655-14660, doi:10.1073/pnas.2532677100.
- 481 Demou, E., H. Visram, D. J. Donaldson, and P. A. Makar (2003), Uptake of water by organic
482 films: the dependence on the film oxidation state, *Atmospheric Environment*, 37, 3529-
483 3537, doi:10.1016/S1352-2310(03)00430-8.
- 484 Dinar, E., A. A. Riziq, C. Spindler, C. Erlick, G. Kiss, and Y. Rudich (2008), The complex
485 refractive index of atmospheric and model humic-like substances (HULIS) retrieved by a
486 cavity ring down aerosol spectrometer (CRD-AS), *Faraday Discussions*, 137, 279-295,
487 doi:10.1039/b703111d.
- 488 Ellison, G. B., A. F. Tuck, and V. Vaida (1999), Atmospheric processing of organic aerosols,
489 *Journal of Geophysical Research-Atmospheres*, 104, 11633-11641,
490 doi:10.1029/1999JD900073.

- 491 Engelhart, G. J., A. Asa-Awuku, A. Nenes, and S. N. Pandis (2008), CCN activity and droplet
492 growth kinetics of fresh and aged monoterpene secondary organic aerosol, *Atmospheric*
493 *Chemistry and Physics*, 8, 3937-3949, doi:10.5194/acp-8-3937-2008.
- 494 Ervens, B., G. Feingold, and S. M. Kreidenweis (2005), Influence of water-soluble organic
495 carbon on cloud drop number concentration, *Journal of Geophysical Research-*
496 *Atmospheres*, 110, D18211, doi:10.1029/2004JD005634.
- 497 Facchini, M. C., M. Mircea, S. Fuzzi, and R. J. Charlson (1999), Cloud albedo enhancement by
498 surface-active organic solutes in growing droplets, *Nature*, 401, 257-259,
499 doi:10.1038/45758.
- 500 Folkers, M., T. F. Mentel, and A. Wahner (2003), Influence of an organic coating on the
501 reactivity of aqueous aerosols probed by the heterogeneous hydrolysis of N₂O₅,
502 *Geophysical Research Letters*, 30, 1644-1647, doi:10.1029/2003GL017168.
- 503 Garland, R. M., M. E. Wise, M. R. Beaver, H. L. Dewitt, A. C. Aiken, J. L. Jimenez, and M. A.
504 Tolbert (2005), Impact of palmitic acid coating on the water uptake and loss of
505 ammonium sulfate particles, *Atmospheric Chemistry and Physics*, 5, 1951-1961,
506 doi:10.5194/acp-5-1951-2005.
- 507 Gerber, H. E., W. A. Hoppel, and T. A. Wojciechowski (1977), Experimental Verification of the
508 Theoretical Relationship Between Size and Critical Supersaturation of Salt Nuclei,
509 *Journal of the Atmospheric Sciences*, 34, 1836-1841, doi:10.1175/1520-
510 0469(1977)034<1836:EVOTTR>2.0.CO;2.
- 511 Gill, P. S., T. E. Graedel, and C. J. Weschler (1983), Organic Films on Atmospheric Aerosol-
512 Particles, Fog Droplets, Cloud Droplets, Raindrops, and Snowflakes, *Reviews of*
513 *Geophysics*, 21, 903-920, doi:10.1029/RG021i004p00903.
- 514 Gilman, J. B., T. L. Eliason, A. Fast, and V. Vaida (2004), Selectivity and stability of organic
515 films at the air-aqueous interface, *Journal of Colloid and Interface Science*, 280, 234-
516 243, doi:10.1016/j.jcis.2004.07.019.
- 517 González-Labrada, E., R. Schmidt, and C. E. DeWolf (2006), Real-time monitoring of the
518 ozonolysis of unsaturated organic monolayers, *Chem. Communications*, 2471-2473,
519 doi:10.1039/b603501a.
- 520 González-Labrada, E., R. Schmidt, and C. E. DeWolf (2007), Kinetic analysis of the ozone
521 processing of an unsaturated organic monolayer as a model of an aerosol surface,
522 *Physical Chemistry Chemical Physics*, 9, 5814-5821, doi:10.1039/b707890k.
- 523 Graham, B., P. Guyon, P. E. Taylor, P. Artaxo, W. Maenhaut, M. M. Glovsky, R. C. Flagan, and
524 M. O. Andreae (2003), Organic compounds present in the natural Amazonian aerosol:
525 Characterization by gas chromatography-mass spectrometry, *Journal of Geophysical*
526 *Research-Atmospheres*, 108, 4766, doi:10.1029/2003JD003990.

527 Hearn, J. D., A. J. Lovett, and G. D. Smith (2005), Ozonolysis of oleic acid particles: evidence
528 for a surface reaction and secondary reactions involving Criegee intermediates, *Physical*
529 *Chemistry Chemical Physics*, 7, 501-511, doi:10.1039/B414472D.

530 Hearn, J. D. and G. D. Smith (2004), Kinetics and product studies for ozonolysis reactions of
531 organic particles using aerosol CIMS, *Journal of Physical Chemistry A*, 108, 10019-
532 10029, doi:10.1021/jp0404145.

533 Hearn, J. D. and G. D. Smith (2005), Measuring rates of reaction in supercooled organic particles
534 with implications for atmospheric aerosol, *Physical Chemistry Chemical Physics*, 7,
535 2549-2551, doi:10.1039/B506424D.

536 Hemming, B. L. and J. H. Seinfeld (2001), On the Hygroscopic Behavior of Atmospheric
537 Organic Aerosols, *Industrial Engineering Chemical Research*, 40, 4162-4171,
538 doi:10.1021/ie000790l.

539 Hung, H. M. and P. Ariya (2007), Oxidation of Oleic Acid and Oleic Acid/Sodium Chloride (aq)
540 Mixture Droplets with Ozone: Changes of Hygroscopicity and Role of Secondary
541 Reactions, *J.Phys.Chem.A.*, 111, 620-632, doi:10.1021/jp0654563.

542 Hung, H. M., Y. Katrib, and S. T. Martin (2005), Products and mechanisms of the reaction of
543 oleic acid with ozone and nitrate radical, *Journal of Physical Chemistry A*, 109, 4517-
544 4530, doi:10.1021/jp0500900.

545 Kanakidou, M., J. H. Seinfeld, S. N. Pandis, I. Barnes, F. J. Dentener, M. C. Facchini, R. Van
546 Dingenen, B. Ervens, A. Nenes, C. J. Nielsen, E. Swietlicki, J. P. Putaud, Y. Balkanski,
547 S. Fuzzi, J. Horth, G. K. Moortgat, R. Winterhalter, C. E. L. Myhre, K. Tsigaridis, E.
548 Vignati, E. G. Stephanou, and J. Wilson (2005), Organic aerosol and global climate
549 modelling: a review, *Atmospheric Chemistry and Physics*, 5, 1053-1123,
550 doi:10.5194/acp-5-1053-2005.

551 Kärcher, B. and T. Koop (2005), The role of organic aerosols in homogeneous ice formation,
552 *Atmospheric Chemistry and Physics*, 5, 703-714, doi:10.5194/acp-5-703-2005.

553 Katrib, Y., G. Biskos, P. R. Buseck, P. Davidovits, J. T. Jayne, M. Mochida, M. E. Wise, D. R.
554 Worsnop, and S. T. Martin (2005a), Ozonolysis of mixed oleic-acid/stearic-acid particles:
555 Reaction kinetics and chemical morphology, *Journal of Physical Chemistry A*, 109,
556 10910-10919, doi:10.1021/jp054714d.

557 Katrib, Y., S. T. Martin, H. M. Hung, Y. Rudich, H. Z. Zhang, J. G. Slowik, P. Davidovits, J. T.
558 Jayne, and D. R. Worsnop (2004), Products and mechanisms of ozone reactions with
559 oleic acid for aerosol particles having core-shell morphologies, *Journal of Physical*
560 *Chemistry A*, 108, 6686-6695, doi:10.1021/jp049759d.

561 Katrib, Y., S. T. Martin, Y. Rudich, P. Davidovits, J. T. Jayne, and D. R. Worsnop (2005b),
562 Density changes of aerosol particles as a result of chemical reaction, *Atmospheric*
563 *Chemistry and Physics*, 5, 275-291, doi:10.5194/acp-5-275-2005.

- 564 Katz, U. and W. C. Kocmond (1973), An Investigation of the Size-Supersaturation Relationship
565 of Soluble Condensation Nuclei, *Journal of the Atmospheric Sciences*, 30, 160-165,
566 doi:10.1175/1520-0469(1973)030<0160:AIOTSS>2.0.CO;2.
- 567 Kawamura, K., Y. Ishimura, and K. Yamazaki (2003), Four years' observations of terrestrial
568 lipid class compounds in marine aerosols from the western North Pacific, *Global*
569 *Biogeochemical Cycles*, 17, 1003, doi:10.1029/2001GB001810.
- 570 Keene, W. C., A. A. P. Pszenny, J. R. Maben, E. Stevenson, and A. Wall (2004), Closure
571 evaluation of size-resolved aerosol pH in the New England coastal atmosphere during
572 summer, *Journal of Geophysical Research-Atmospheres*, 109, D23202,
573 doi:10.1029/2004JD004801.
- 574 King, M. D., A. R. Rennie, K. C. Thompson, F. N. Fisher, C. C. Dong, R. K. Thomas, C. Pfrang,
575 and A. V. Hughes (2009), Oxidation of oleic acid at the air-water interface and its
576 potential effects on cloud critical supersaturations, *Physical Chemistry Chemical Physics*,
577 11, 7699-7707, doi:10.1039/b906517b.
- 578 King, M. D., K. C. Thompson, and A. D. Ward (2004), Laser Tweezers Raman Study of
579 Optically Trapped Aerosol Droplets of Seawater and Oleic Acid Reacting with Ozone:
580 Implications for Cloud-Droplet Properties, *Journal of the American Chemical Society*,
581 126, 16710-16711, doi:10.1021/ja044717o.
- 582 Knopf, D. A., L. M. Anthony, and A. K. Bertram (2005), Reactive uptake of O₃ by
583 multicomponent and multiphase mixtures containing oleic acid, *Journal of Physical*
584 *Chemistry A*, 109, 5579-5589, doi:10.1021/jp0512513.
- 585 Kokkola, H., R. Sorjamaa, A. Peräniemi, T. Raatikainen, and A. Laaksonen (2006), Cloud
586 formation of particles containing humic-like substances, *Geophysical Research Letters*,
587 33, doi:10.1029/2006GL026107.
- 588 Kumar, P. P., K. Broekhuizen, and J. P. D. Abbatt (2003), Organic acids as cloud condensation
589 nuclei: Laboratory studies of highly soluble and insoluble species, *Atmospheric*
590 *Chemistry and Physics*, 3, 509-520, doi:10.5194/acp-3-509-2003.
- 591 Lance, S., J. Medina, J. N. Smith, and A. Nenes (2006), Mapping the Operation of the DMT
592 Continuous Flow CCN Counter, *Aerosol Science and Technology*, 40, 242-254,
593 doi:10.1080/02786820500543290.
- 594 Langmuir, I. (1917), The Shapes of Group Molecules Forming the Surfaces of Liquids,
595 *Proceedings of the National Academy of Sciences of the United States of America*, 3, 251-
596 257.
- 597 Lass, K., J. Kleber, and F. Gernot (2010), Vibrational sum-frequency generation as a probe for
598 composition, chemical reactivity, and film formation dynamics of the sea surface
599 nanolayer, *Limnology and Oceanography: Methods*, 8, 216-228,
600 doi:10.4319/lom.2010.8.216.

- 601 Lee, A. K. Y. and C. K. Chan (2007), Single particle Raman spectroscopy for investigating
602 atmospheric heterogeneous reactions of organic aerosols, *Atmospheric Environment*, 41,
603 4611-4621, doi:10.1016/j.atmosenv.2007.03.040.
- 604 Limbeck, A. and H. Puxbaum (1999), Organic acids in continental background aerosols,
605 *Atmospheric Environment*, 33, 1847-1852, doi:10.1016/S1352-2310(98)00347-1.
- 606 Malm, W. C. and S. M. Kreidenweis (1997), The Effects of Models of Aerosol Hygroscopicity
607 on the Apportionment of Extinction, *Atmospheric Environment*, 31, 1965-1976,
608 doi:10.1016/S1352-2310(96)00355-X.
- 609 McIntire, T. M., O. S. Ryder, P. L. Gassman, Z. Zhu, S. Ghosal, and B. J. Finlayson-Pitts (2010),
610 Why ozonolysis may not increase the hydrophilicity of particles, *Atmospheric*
611 *Environment*, 939-944, doi:10.1016/j.atmosenv.2009.11.009.
- 612 McNeill, V. F., G. M. Wolfe, and J. A. Thornton (2007), The Oxidation of Oleate in Submicron
613 Aqueous Salt Aerosols: Evidence of a Surface Process, *J.Phys.Chem.A.*, 111, 1073-1083,
614 doi:10.1021/jp066233f.
- 615 McNeill, V. F., J. Patterson, G. M. Wolfe, and J. A. Thornton (2006), The effect of varying
616 levels of surfactant on the reactive uptake of N₂O₅ to aqueous aerosol, *Atmospheric*
617 *Chemistry and Physics*, 6, 1635-1644, doi:10.5194/acp-6-1635-2006.
- 618 Mircea, M., M. C. Facchini, S. Decesari, F. Cavalli, L. Emblico, S. Fuzzi, A. Vestin, J. Rissler,
619 E. Swietlicki, G. Frank, M. O. Andreae, W. Maenhaut, Y. Rudich, and P. Artaxo (2005),
620 Importance of the organic aerosol fraction for modeling aerosol hygroscopic growth and
621 activation: a case study in the Amazon Basin, *Atmospheric Chemistry and Physics*, 5,
622 3111-3126, doi:10.5194/acp-5-3111-2005.
- 623 Moise, T. and Y. Rudich (2000), Reactive uptake of ozone by proxies for organic aerosols:
624 Surface versus bulk processes, *Journal of Geophysical Research-Atmospheres*, 105,
625 14667-14676, doi:10.1029/2000JD900071.
- 626 Moise, T. and Y. Rudich (2002), Reactive uptake of ozone by aerosol-associated unsaturated
627 fatty acids: Kinetics, mechanism, and products, *Journal of Physical Chemistry A*, 106,
628 6469-6476, doi:10.1021/jp025597e.
- 629 Moore, R. H., E. D. Ingall, A. Sorooshian, and A. Nenes (2008), Molar mass, surface tension,
630 and droplet growth kinetics of marine organics from measurements of CCN activity,
631 *Geophysical Research Letters*, 35, doi:10.1029/2008GL033350.
- 632 Moore, R. H., A. Nenes, and J. Medina (2010), Scanning Mobility CCN Analysis - A Method for
633 Fast Measurements of Size-Resolved CCN Distributions and Activation Kinetics, *Aerosol*
634 *Science and Technology*, 44, 861-871, doi:10.1080/02786826.2010.498715.
- 635 Morris, J. W., P. Davidovits, J. T. Jayne, J. L. Jimenez, Q. Shi, C. E. Kolb, D. R. Worsnop, W. S.
636 Barney, and G. Cass (2002), Kinetics of submicron oleic acid aerosols with ozone: A

637 novel aerosol mass spectrometric technique, *Geophysical Research Letters*, 29,
638 doi:10.1029/2002GL014692.

639 Nash, D. G., M. P. Tolocka, and T. Baer (2005), The uptake of O₃ by myristic acid-oleic acid
640 mixed particles: evidence for solid surface layers, *Physical Chemistry Chemical Physics*,
641 8, 4468-4475, doi:10.1039/b609855j.

642 Nenes, A., R. J. Charlson, M. C. Facchini, M. Kulmala, A. Laaksonen, and J. H. Seinfeld (2002),
643 Can chemical effects on cloud droplet number rival the first indirect effect?, *Geophysical*
644 *Research Letters*, 29, 1848, doi:10.1029/2002GL015295.

645 Novakov, T. and J. E. Penner (1993), Large contribution of organic aerosols to cloud-
646 condensation-nuclei concentrations, *Nature*, 365, 823-826, doi:10.1038/365823a0.

647 Padro, L. T., A. Asa-Awuku, R. Morrison, and A. Nenes (2007), Inferring thermodynamic
648 properties from CCN activation experiments: single-component and binary aerosols,
649 *Atmospheric Chemistry and Physics*, 7, 5263-5274, doi:10.5194/acp-7-5263-2007.

650 Petters, M. D. and S. M. Kreidenweis (2007), A single parameter representation of hygroscopic
651 growth and cloud condensation nucleus activity, *Atmospheric Chemistry and Physics*, 7,
652 1961-1971, doi:10.5194/acp-7-1961-2007.

653 Pfrang, C., M. Shiraiwa, and C. Pöschl (2010), Coupling aerosol surface and bulk chemistry with
654 a kinetic double layer model (K2-SUB): oxidation of oleic acid by ozone, *Atmospheric*
655 *Chemistry and Physics*, 10, 4537-4557, doi:10.5194/acp-10-4537-2010.

656 Reynolds, J. C., D. J. Last, M. McGillen, A. Nijs, A. B. Horn, C. Percival, L. J. Carpenter, and
657 A. C. Lewis (2006), Structural Analysis of Oligomeric Molecules Formed from the
658 Reaction Products of Oleic Acid Ozonolysis, *Environmental Science & Technology*, 40,
659 6674-6681, doi:10.1021/es060842p.

660 Riddick, J. A., W. B. Bunger, and T. K. Sakano (1986), *Organic Solvents: Physical Properties*
661 *and Methods of Purification*, Wiley & Sons.

662 Rideal, E. K. (1925), On the influence of surface films in the evaporation of water, *Journal of*
663 *Physical Chemistry*, 29, 1585-1588, doi:10.1021/j150258a011.

664 Roberts, G. C. and A. Nenes (2005), A continuous-flow streamwise thermal-gradient CCN
665 chamber for atmospheric measurements, *Aerosol Science and Technology*, 39, 206-221,
666 doi:10.1080/027868290913988.

667 Robinson, A. L., N. M. Donahue, and W. F. Rogge (2006), Photochemical oxidation and changes
668 in molecular composition of organic aerosol in the regional context, *Journal of*
669 *Geophysical Research-Atmospheres*, 111, D03302, doi:10.1029/2005JD006265.

670 Rogge, W. F., L. M. Hildemann, M. A. Mazurek, G. R. Cass, and B. R. T. Simonelt (1991),
671 Sources of Fine Organic Aerosol .1. Charbroilers and Meat Cooking Operations,
672 *Environmental Science & Technology*, 25, 1112-1125, doi:10.1021/es00018a015.

- 673 Rubel, G. O. and J. W. Gentry (1984), Measurement of the Kinetics of Solution Droplets in the
674 Presence of Adsorbed Monolayers: Determination of Water Accommodation
675 Coefficients, *Journal of Physical Chemistry*, 88, 3142-3148, doi:10.1021/j150658a046.
- 676 Rudich, Y., I. Benjamin, R. Naaman, E. Thomas, S. Trakhtenberg, and R. Ussyshkin (2000),
677 Wetting of Hydrophobic Organic Surfaces and Its Implications to Organic Aerosols in the
678 Atmosphere, *J.Phys.Chem.A.*, 104, 5238-5245, doi:10.1021/jp994203p.
- 679 Rudich, Y., N. M. Donahue, and T. F. Mentel (2007), Aging of Organic Aerosol: Bridging the
680 Gap Between Laboratory and Field Studies, *Annual Review of Physical Chemistry*, 48,
681 321-352, doi:10.1146/annurev.physchem.58.032806.104432.
- 682 Sage, A. M., A. Weitkamp, A. L. Robinson, and N. M. Donahue (2009), Reactivity of oleic acid
683 in organic particles: changes in oxidant uptake and reaction stoichiometry with particle
684 oxidation, *Physical Chemistry Chemical Physics*, 11, 7951-7962, doi:10.1039/b904285g.
- 685 Saxena, P. and L. M. Hildemann (1997), Water Absorption by Organics: Survey of Laboratory
686 Evidence and Evaluation of UNIFAC for Estimating Water Activity, *Environmental
687 Science & Technology*, 31, 3318-3324, doi:10.1021/es9703638.
- 688 Schauer, J. J., M. J. Kleeman, G. R. Cass, and B. R. T. Simoneit (2002), Measurement of
689 emissions from air pollution sources. 4. C₁-C₂₇ organic compounds from cooking with
690 seed oils, *Environmental Science & Technology*, 36, 567-575, doi:10.1021/es002053m.
- 691 Schauer, J. J., W. F. Rogge, L. M. Hildemann, M. A. Mazurek, and G. R. Cass (1996), Source
692 apportionment of airborne particulate matter using organic compounds as tracers,
693 *Atmospheric Environment*, 30, 3837-3855, doi:10.1016/j.atmosenv.2007.10.069.
- 694 Schofield, R. K. and E. K. Rideal (1926), The Kinetic Theory of Surface Films - Part II.
695 Gaseous, Expanded, and Condensed Films., *Proceedings of the Royal Society*, 110A,
696 167-177, doi:10.1098/rspa.1926.0009.
- 697 Shilling, J. E., S. M. King, M. Mochida, D. R. Worsnop, and S. T. Martin (2007), Mass spectral
698 evidence that small changes in composition caused by oxidative aging processes alter
699 aerosol CCN properties, *Journal of Physical Chemistry A*, 111, 3358-3368,
700 doi:10.1021/jp068822r.
- 701 Shulman, M. L., M. C. Jacobson, R. J. Carlson, R. E. Synovec, and T. E. Young (1996),
702 Dissolution behavior and surface tension effects of organic compounds in nucleating
703 cloud droplets, *Geophysical Research Letters*, 23, 277-280, doi:10.1029/95GL03810.
- 704 Simoneit, B. R. T., M. Kobayashi, M. Mochida, K. Kawamura, M. Lee, H. J. Lim, B. J. Turpin,
705 and Y. Komazaki (2004), Composition and major sources of organic compounds of
706 aerosol particulate matter sampled during the ACE-Asia campaign, *Journal of
707 Geophysical Research-Atmospheres*, 109, doi:10.1029/2004JD004598.
- 708 Smith, G. D., E. Woods, C. L. DeForest, T. Baer, and R. E. Miller (2002), Reactive uptake of
709 ozone by oleic acid aerosol particles: Application of single-particle mass spectrometry to

710 heterogeneous reaction kinetics, *Journal of Physical Chemistry A*, 106, 8085-8095,
711 doi:10.1021/jp020527t.

712 Sorjamaa, R. and A. Laaksonen (2006), The influence of surfactant properties on critical
713 supersaturations of cloud condensation nuclei, *Journal of Aerosol Science*, 37, 1730-
714 1736, doi:10.1016/j.jaerosci.2006.07.004.

715 Sorjamaa, R., B. Svenningsson, T. Raatikainen, S. Henning, M. Bilde, and A. Laaksonen (2004),
716 The role of surfactants in Kohler theory reconsidered, *Atmospheric Chemistry and*
717 *Physics*, 4, 2107-2117, doi:10.5194/acp-4-2107-2004.

718 Stephanou, E. G. and N. Stratigakis (1993), Oxocarboxylic and α,ω -Dicarboxylic Acids:
719 Photooxidation Products of Biogenic Unsaturated Fatty Acids Present in Urban Aerosols,
720 *Environmental Science & Technology*, 27, 1403-1407, doi:10.1021/es00044a016.

721 ten Brink, H. M. (1998), Reactive uptake of HNO₃ and H₂SO₄ in sea-salt (NaCl) particles,
722 *Journal of Aerosol Science*, 29, 57-64, doi:10.1016/S0021-8502(97)00460-6.

723 Thornberry, T. and J. P. D. Abbatt (2004), Heterogeneous reaction of ozone with liquid
724 unsaturated fatty acids: detailed kinetics and gas-phase product studies, *Physical*
725 *Chemistry Chemical Physics*, 6, 84-93, doi:10.1039/b310149e.

726 Thornton, J. A. and J. P. D. Abbatt (2005), N₂O₅ Reaction on Sub-micron Sea Salt Aerosol:
727 Effect of Surface Active Organics, *Journal of Physical Chemistry A*, 109, 10004-10012,
728 doi:10.1021/jp054183t.

729 Tuckermann, R. (2007), Surface tension of aqueous solutions of water-soluble organic and
730 inorganic compounds, *Atmospheric Environment*, 41, 6265-6275,
731 doi:10.1016/j.atmosenv.2007.03.051.

732 Tuckermann, R. and H. K. Cammenga (2004), The surface tension of aqueous solutions of some
733 atmospheric water-soluble organic compounds, *Atmospheric Environment*, 38, 6135-
734 6138, doi:10.1016/j.atmosenv.2004.08.005.

735 Turpin, B. J. and H. J. Lim (2001), Species Contributions to PM_{2.5} Mass Concentrations:
736 Revisiting Common Assumptions for Estimating Organic Mass, *Aerosol Science and*
737 *Technology*, 35, 602-610, doi:10.1080/02786820119445.

738 Vesna, O., M. Sax, M. Kalberer, A. Gaschen, and M. Ammann (2009), Product study of oleic
739 acid ozonolysis as function of humidity, *Atmospheric Environment*, 43, 3662-3669,
740 doi:10.1016/j.atmosenv.2009.04.047.

741 Vesna, O., S. Sjogren, E. Weingartner, V. Samburova, M. Kalberer, H. W. Gäggeler, and M.
742 Ammann (2008), Changes of fatty acid aerosol hygroscopicity induced by ozonolysis,
743 *Atmospheric Chemistry and Physics*, 8, 4683-4690, doi:10.5194/acp-8-4683-2008.

- 744 Voss, L. F., M. F. Bazerbashi, C. P. Beekman, C. M. Hadad, and H. C. Allen (2007), Oxidation
745 of oleic acid at air/liquid interfaces, *Journal of Geophysical Research-Atmospheres*, 112,
746 doi:10.1029/2006JD007677.
- 747 Voss, L. F., C. M. Hadad, and H. C. Allen (2006), Competition between Atmospherically
748 Relevant Fatty Acid Monolayers at the Air/Water Interface, *Journal of Physical*
749 *Chemistry B*, 110, 19487-19490, doi:10.1021/jp062595b.
- 750 Wadia, Y., D. J. Tobias, R. Stafford, and B. J. Finlayson-Pitts (2000), Real-time monitoring of
751 the kinetics and gas-phase products of the reaction of ozone with an unsaturated
752 phospholipid at the air-water interface, *Langmuir*, 16, 9321-9330,
753 doi:10.1021/la0006622.
- 754 Washburn, E. W. (2003), International Critical Tables Of Numerical Data, Physics, Chemistry
755 and Technology.
- 756 Yue, Z. W. and M. P. Fraser (2004), Polar organic compounds measured in fine particulate
757 matter during TexAQS 2000, *Atmospheric Environment*, 38, 3253-3261,
758 doi:10.1016/j.atmosenv.2004.03.014.
- 759 Zahardis, J., B. W. LaFranchi, and G. A. Petrucci (2005), Photoelectron resonance capture
760 ionization-aerosol mass spectrometry of the ozonolysis products of oleic acid particles:
761 Direct measure of higher molecular weight oxygenates, *Journal of Geophysical*
762 *Research-Atmospheres*, 110, D08307, doi:10.1029/2004JD005336.
- 763 Zahardis, J., B. W. LaFranchi, and G. A. Petrucci (2006a), Direct observation of polymerization
764 in the oleic acid-ozone heterogeneous reaction system by photoelectron resonance
765 capture ionization aerosol mass spectrometry, *Atmospheric Environment*, 40, 1661-1670,
766 doi:10.1016/j.atmosenv.2005.10.065.
- 767 Zahardis, J., B. W. LaFranchi, and G. A. Petrucci (2006b), The heterogeneous reaction of
768 particle-phase methyl esters and ozone elucidated by photoelectron resonance capture
769 ionization: Direct products of ozonolysis and secondary reactions leading to the
770 formation of ketones, *International Journal of Mass Spectrometry*, 253, 38-47,
771 doi:10.1016/j.ijms.2006.02.010.
- 772 Zahardis, J. and G. A. Petrucci (2007), The oleic acid-ozone heterogeneous reaction system:
773 products, kinetics, secondary chemistry, and atmospheric implications of a model system
774 - a review, *Atmospheric Chemistry and Physics*, 7, 1237-1274, doi:10.5194/acp-7-1237-
775 2007.
- 776 Zhang, Q., J. L. Jimenez, D. R. Worsnop, and M. Canagaratna (2007), A case study of urban
777 particle acidity and its influence on secondary organic aerosol, *Environmental Science &*
778 *Technology*, 41, 3213-3219, doi: 10.1021/es061812j.
- 779 Ziemann, P. J. (2005), Aerosol products, mechanisms, and kinetics of heterogeneous reactions of
780 ozone with oleic acid in pure and mixed particles, *Faraday Discussions*, 130, 469-490,
781 doi:10.1039/b417502f.

782

783 *Figure Captions*

784

785 **Figure 1.** Experimental setup. The solutions were atomized, and combined with humidified N₂;
786 this flow entered the flow tube reactor simultaneously with O₃ in an N₂ stream. The reactor
787 effluent passed through a drier before being characterized with a Differential Mobility Analyzer
788 (DMA), Condensation Particle Counter (CPC) and a Continuous Flow Streamwise Thermal
789 Gradient CCN Chamber (CFSTGC).

790 **Figure 2.** CCN activity of SO/NaCl particles. Particles generated from solutions containing 0.001
791 M or 0.01 M SO mixed with 0.05 M NaCl were exposed to O₃ concentrations ranging between
792 0.2-1ppm in an aerosol flow tube reactor. Instrument supersaturation is shown as a function of
793 A) critical dry diameter and B) activated wet diameter. In both plots, the red dots represent the
794 salt calibration, and the red lines are guides to the eye. In panel A) an inset focuses on higher
795 supersaturations. In panel B) the gray lines indicate the standard deviation in the salt calibration.

796 **Figure 3.** CCN activity of SO/Na₂SO₄ particles. Particles generated from solutions containing
797 0.001 M or 0.01 M SO mixed with 0.06 M Na₂SO₄, were oxidized with 1 ppm O₃ in an aerosol
798 flow tube reactor. Instrument supersaturation is shown as a function of A) critical dry diameter
799 and B) activated wet diameter. In both plots, the red dots represent the salt calibration, and the
800 red lines are guides to the eye. In panel A) an inset focuses on higher supersaturations. In panel
801 B) the gray lines indicate the standard deviation in the salt calibration.

802 **Figure 4.** CCN activity of SO/NaCl particles exposed to H₂SO₄. Particles generated from
803 solutions containing 0.001 M or 0.01 M SO mixed with 0.05 M NaCl were oxidized with 1 ppm
804 O₃ in a flow tube reactor. Instrument supersaturation is shown as a function of A) critical dry
805 diameter and B) activated wet diameter. In both plots, the red dots represent the salt calibration,
806 and the red lines are guides to the eye. In panel A) an inset focuses on higher supersaturations. In
807 panel B) the gray lines indicate the standard deviation in the salt calibration.

808 **Figure 5.** CCN activity of SO/Na₂SO₄ particles exposed to H₂SO₄. Particles generated from
809 solutions containing 0.001 M or 0.01 M SO mixed with 0.06 M Na₂SO₄ were oxidized with 1
810 ppm O₃ in a flow tube reactor. Instrument supersaturation is shown as a function of A) critical
811 dry diameter and B) activated wet diameter. In both plots, the red dots represent the salt
812 calibration, and the red lines are guides to the eye. In panel A) an inset focuses on higher
813 supersaturations. In panel B) the gray lines indicate the standard deviation in the salt calibration.

814 *Tables*

815

816 **Table 1.** KTA Parameters used before and after oxidation, based on in-particle concentrations of
817 0.176 or 1.76 M oleate and either 8.6 M NaCl or 10.6 M Na₂SO₄ .

818

| KTA Parameters | 0.176 M | | | | 1.76 M | | | |
|------------------------------|----------------------|---------------------------------|----------------------------------|---------------------------------|----------------------|---------------------------------|------------------------------|---------------------------------|
| | Before Oxidation | | After Oxidation (0.2-1ppm) | | Before Oxidation | | After Oxidation (1ppm) | |
| | NaCl | Na ₂ SO ₄ | NaCl | Na ₂ SO ₄ | NaCl | Na ₂ SO ₄ | NaCl | Na ₂ SO ₄ |
| ϵ_o | 0.19 | 0.09 | 0.12 | 0.05 | 0.71 | 0.50 | 0.57 | 0.35 |
| M_o (g/mol) | 282.46 | | 169.93 | | 282.46 | | 169.93 | |
| ρ_o (g/m ³) | 8.95x10 ⁵ | | 9.94x10 ⁵ | | 8.95x10 ⁵ | | 9.94x10 ⁵ | |
| u_o | 2 | | 2 | | 2 | | 2 | |

819

820 **Table 2.**Inferred surface tension for unacidified aerosols from eqns. (3-5), assuming in-particle
821 concentrations of 0.176 or 1.76 Moleate in either 8.6 M NaCl or 10.6 M Na₂SO₄.

822

| | σ (mN/m) [0.176 M] | | | σ (mN/m) [1.76 M] | | |
|---------------------------------|---------------------------|------------------------------|--------------------------------|--------------------------|------------------------------|--------------------------------|
| | Before Oxidation | After Oxidation (1ppm) | After Oxidation (0.2ppm) | Before Oxidation | After Oxidation (1ppm) | After Oxidation (0.2ppm) |
| | NaCl | 68.1 | 70.5 | 71.7 | 57.5 | 64.4 |
| Na ₂ SO ₄ | 73.9 | 74.8 | - | 63.7 | 69.9 | - |

823

824 **Table 3.**Inferred surface tension for acidified aerosols from eqns. (3-5), assuming in-particle
825 concentrations of 0.176 or 1.76 M oleate in either 8.6 M NaCl or 10.6 M Na₂SO₄.

826

| | σ (mN/m) [0.176 M] | | σ (mN/m) [1.76 M] | |
|---------------------------------|---------------------------|---------------------------|--------------------------|---------------------------|
| | Before Oxidation | After Oxidation (1ppm) | Before Oxidation | After Oxidation (1ppm) |
| NaCl | 69.1 | 72.9 | 55.5 | 67.4 |
| Na ₂ SO ₄ | 72.4 | 74.8 | 66.1 | 74.8 |

827

828

829

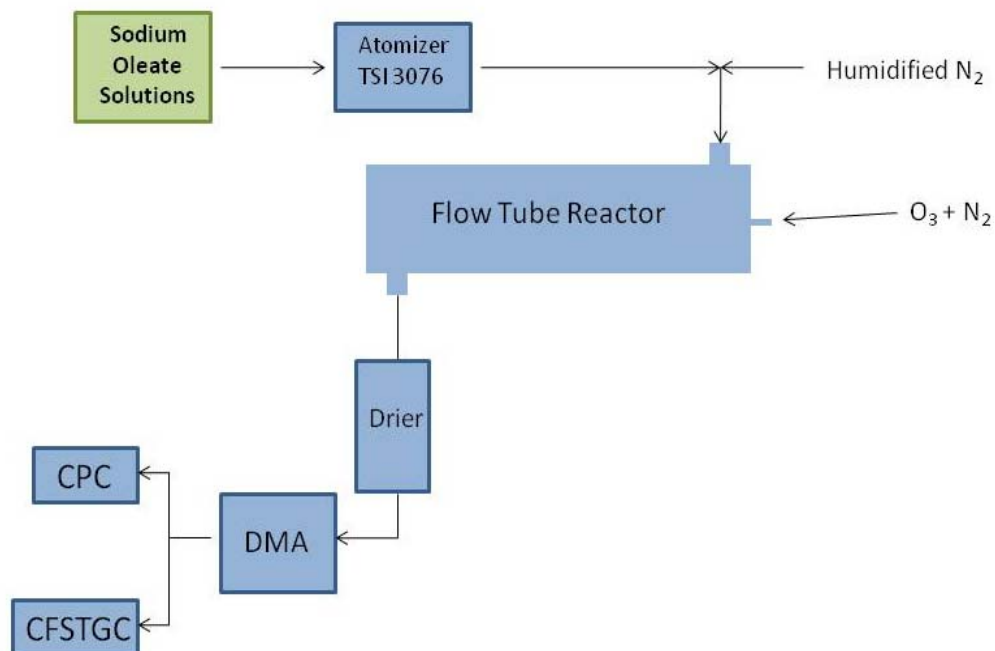
830

831

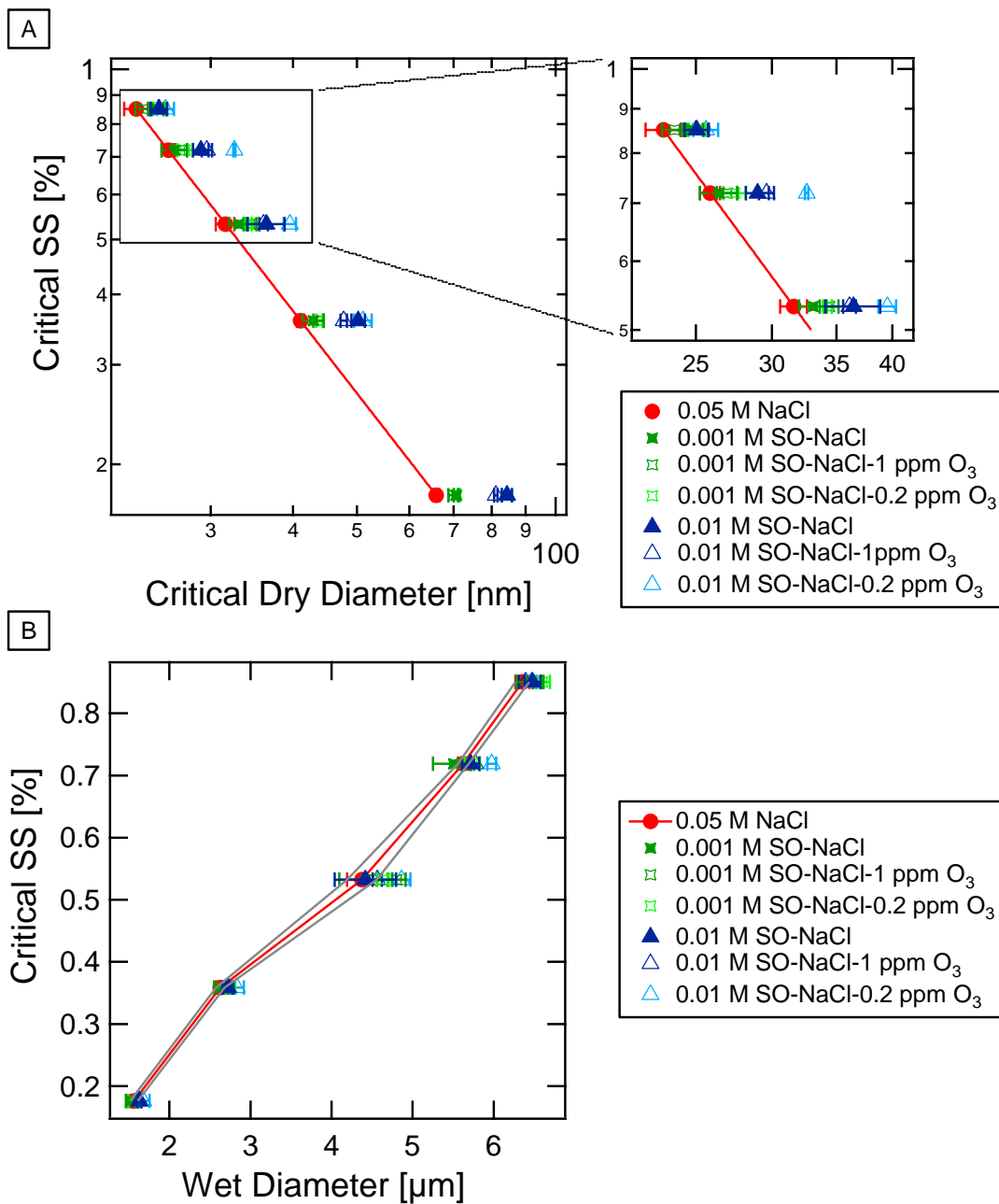
832

833 **Figures**

834



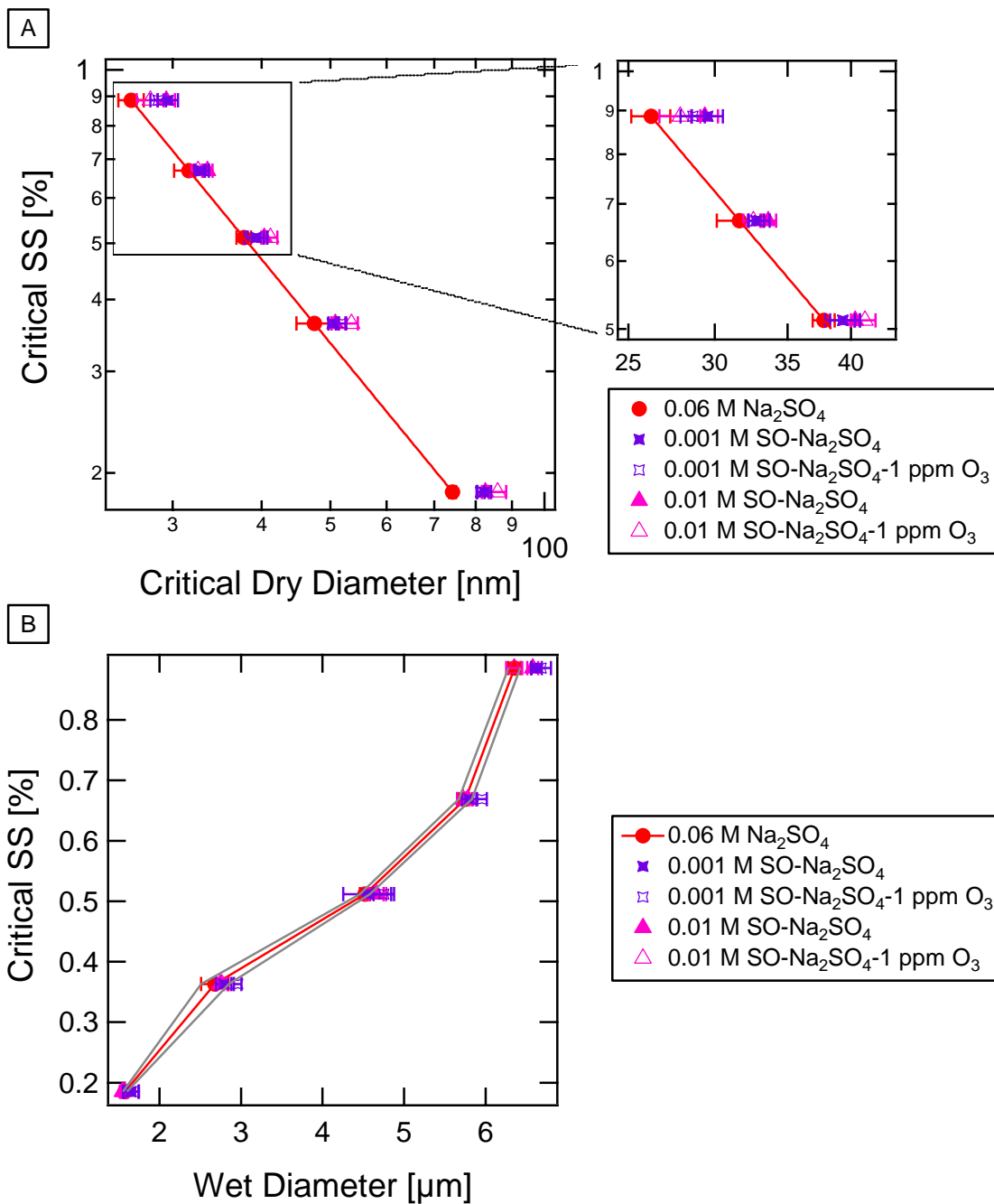
835
 836 **Figure 1.** Experimental setup. The solutions were atomized, and combined with humidified N₂;
 837 this flow entered the flow tube reactor simultaneously with O₃ in an N₂ stream. The reactor
 838 effluent passed through a drier before being characterized with a Differential Mobility Analyzer
 839 (DMA), Condensation Particle Counter (CPC) and a Continuous Flow Streamwise Thermal
 840 Gradient CCN Chamber (CFSTGC).



841

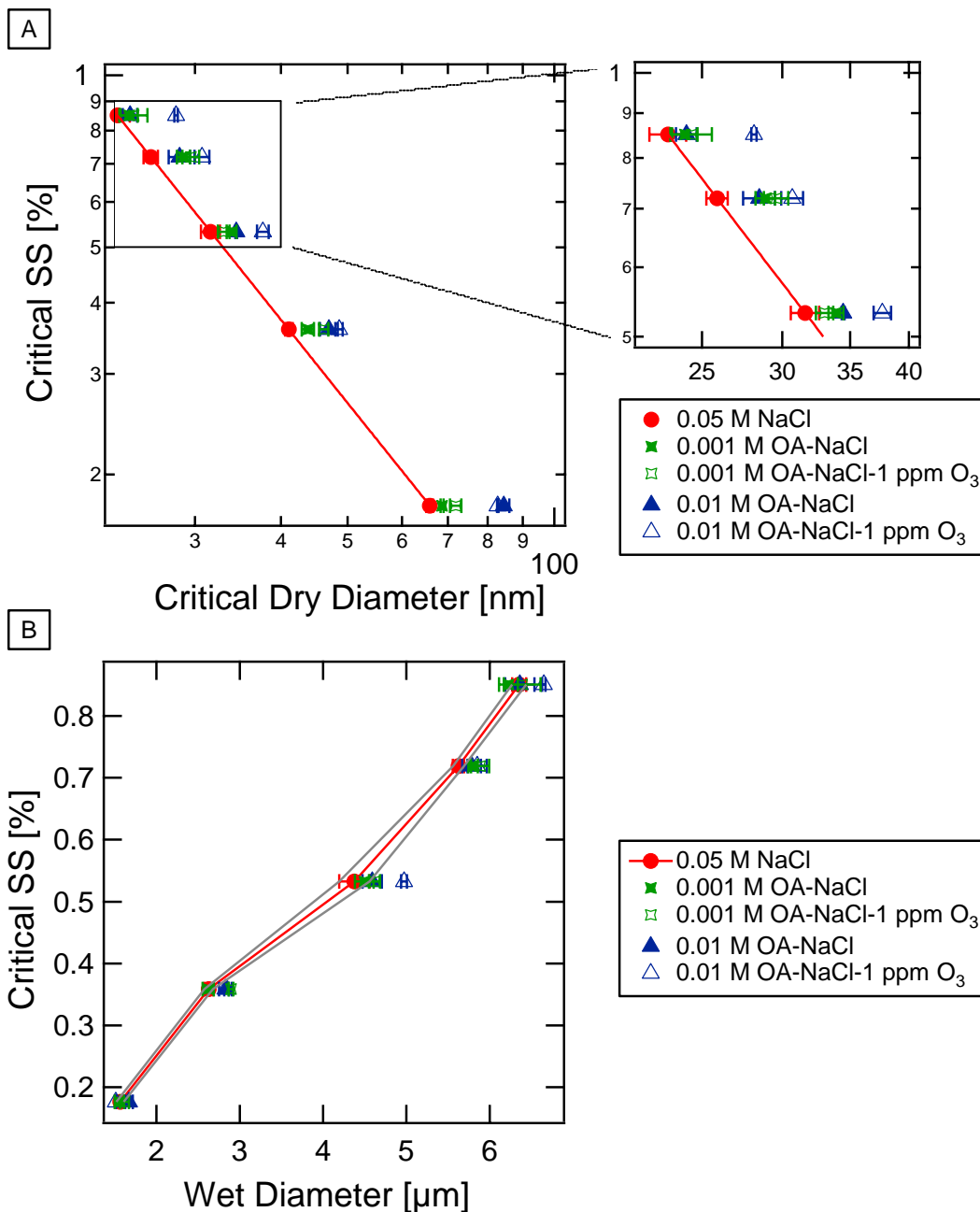
842 **Figure 2.**CCN activity of SO/NaCl particles. Particles generated from solutions containing 0.001
 843 M or 0.01 M SO mixed with 0.05 M NaCl were exposed to O₃ concentrations ranging between
 844 0.2-1ppm in an aerosol flow tube reactor. Instrument supersaturation is shown as a function of
 845 A) critical dry diameter and B) activated wet diameter. In both plots, the red dots represent the
 846 salt calibration, and the red lines are guides to the eye. In panel A) an inset focuses on higher
 847 supersaturations. In panel B) the gray lines indicate the standard deviation in the salt calibration.

848



849

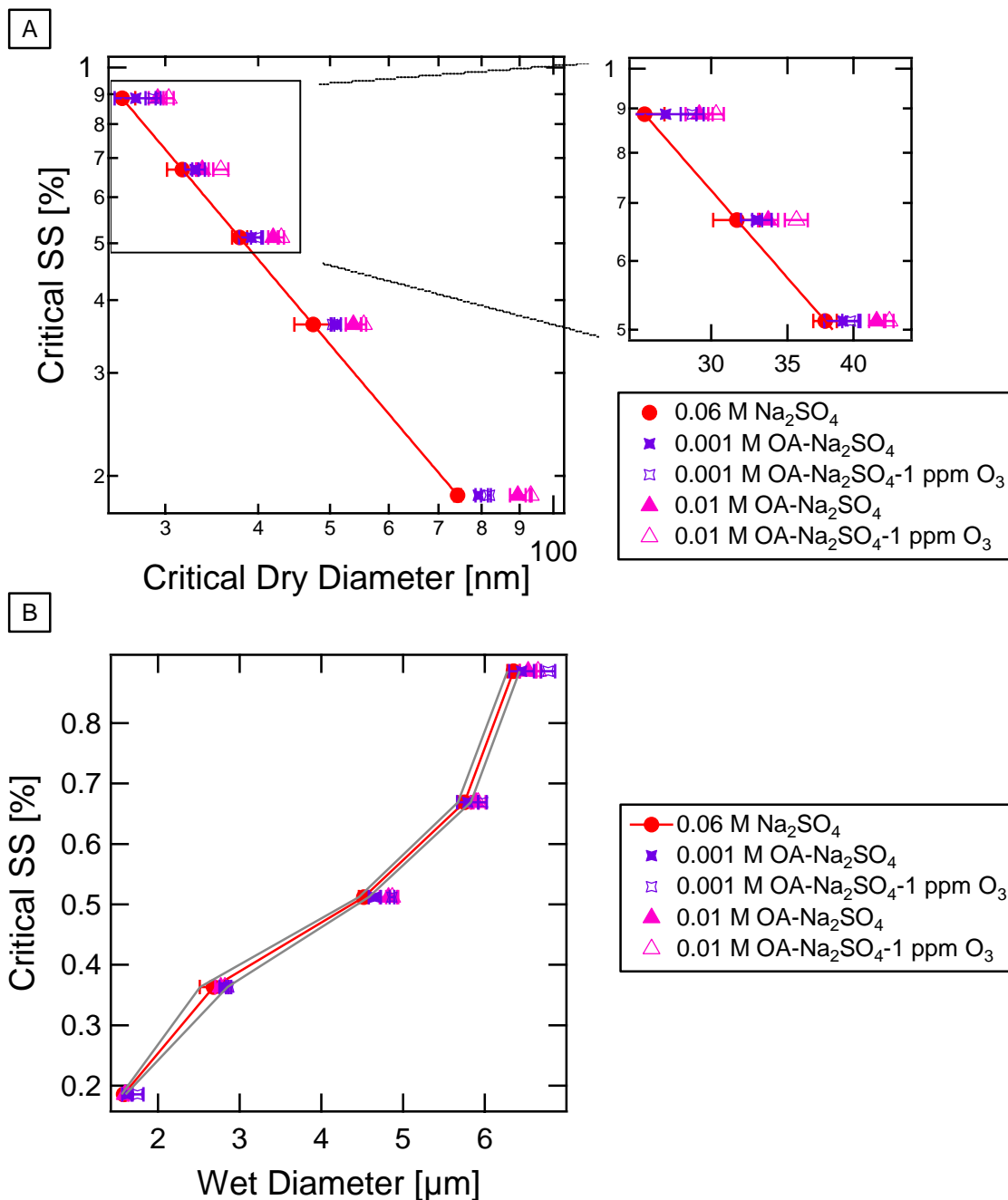
850 **Figure 3.** CCN activity of SO/Na₂SO₄ particles. Particles generated from solutions containing
 851 0.001 M or 0.01 M SO mixed with 0.06 M Na₂SO₄, were oxidized with 1 ppm O₃ in an aerosol
 852 flow tube reactor. Instrument supersaturation is shown as a function of A) critical dry diameter
 853 and B) activated wet diameter. In both plots, the red dots represent the salt calibration, and the
 854 red lines are guides to the eye. In panel A) an inset focuses on higher supersaturations. In panel
 855 B) the gray lines indicate the standard deviation in the salt calibration.



856

857 **Figure 4.** CCN activity of SO/NaCl particles exposed to H₂SO₄. Particles generated from
 858 solutions containing 0.001 M or 0.01 M SO mixed with 0.05 M NaCl were oxidized with 1 ppm
 859 O₃ in a flow tube reactor. Instrument supersaturation is shown as a function of A) critical dry
 860 diameter and B) activated wet diameter. In both plots, the red dots represent the salt calibration,
 861 and the red lines are guides to the eye. In panel A) an inset focuses on higher supersaturations. In
 862 panel B) the gray lines indicate the standard deviation in the salt calibration.

863



864

865 **Figure 5.** CCN activity of SO/Na₂SO₄ particles exposed to H₂SO₄. Particles generated from
 866 solutions containing 0.001 M or 0.01 M SO mixed with 0.06 M Na₂SO₄, were oxidized with 1
 867 ppm O₃ in an aerosol flow tube reactor. Instrument supersaturation is shown as a function of A)
 868 critical dry diameter and B) activated wet diameter. In both plots, the red dots represent the salt
 869 calibration, and the red lines are guides to the eye. In panel A) an inset focuses on higher
 870 supersaturations. In panel B) the gray lines indicate the standard deviation in the salt calibration.

871